CONSTRAINED TOTAL VARIATION MINIMIZATION FOR PHOTOACOUSTIC TOMOGRAPHY

S. M. Akramus Salehin *Thushara D. Abhayapala*

College of Engineering and Computer Science
Australian National University, Canberra, ACT 0200, Australia

ABSTRACT

Similar to computed tomography, the images from photoacoustic tomography are piecewise smooth and reconstructions can be enhanced by applying Total Variation (TV) minimization. Also, the photoacoustic image must satisfy both the data fidelity and a non negativity constraint. This paper proposes a constrained TV minimization formulation in the Fourier Bessel domain which has the advantage of reducing the dimension of the fidelity constraint and the projection onto this constraint can be performed by a simple projection onto the l_2 ball. The TV minimization post processing improves the quality of images reconstructed and recovers the lost, low frequency information when sensor lower frequency limit is higher than zero.

Index Terms— Tomography, Thermoacoustic, Projected subgradient, Fourier Bessel series

1. INTRODUCTION

Photoacoustic Tomography (PAT) consists of solving an inverse problem to reconstruct images from recorded acoustic waves generated within the sample of interest. This imaging modality illuminates the sample with a short electromagnetic (EM) pulse. Upon absorption of this EM energy, the tissue expands and releases an acoustic wave. The solution to the photoacoustic inverse problem calculates the initial pressure distribution. Cancer detection is one of the most important applications of this imaging modality, together with small animal and molecular imaging.

The TV functional reconstructs images that have a spatially sparse gradient consisting of large constant regions and sharp edges. Therefore, the Total Variation objective allows to separate different objects clearly which is particularly important for tomographic imaging. The idea that medical images are often piecewise constant has been recognized before and incorporated into a TV minimization problem by Delaney and Bresler [1].

This paper proposes a constrained TV formulation for photoacoustic tomography in the Fourier Bessel domain (with Frequency-Radial duality (F-R) based inversion [2, 3]). An unconstrained formulation is easier to implement but reconstructions are dependent on the value of the Lagrangian parameter. Moreover, a projected, subgradient based method is devised to solve the proposed optimization problem. The proposed method is designed to handle the large data sets present for photoacoustic tomography hence interior point methods cannot be used. Further, by working in the Fourier Bessel domain, the dimension of the fidelity constraint is reduced and the projection onto this constraint does not require solving a computationally expensive second order cone program (SOCP). Additionally, it is either difficult or impossible to apply TV minimization to other photoacoustic inversion methods.

This paper is organized as follows: The next section describes a constrained TV formulation for PAT. Section 3 summarizes the operation of the F-R based reconstruction method, section 4 provides the TV formulation in the Fourier Bessel domain, outlining its advantages. The next section describes the subgradient method for solving the TV minimization problem and section 6 describes numerical experiments performed. Section 7 provides a summary of the main ideas.

2. CONSTRAINED TV MODEL FOR PAT

This paper considers the 2D photoacoustic inverse problem where a circular array of sensors are uniformly placed at a radius of r_s, the measured pressure $p(\phi_s, k)$ at an angular position ϕ_s is [2, 3]

$$p(\phi_s, k) = -ikc \int_0^{2\pi} \int_0^{r_0} S(\boldsymbol{r}) G(k; (r_s, \phi_s), \boldsymbol{r})\, r \mathrm{d}r\, \mathrm{d}\phi \tag{1}$$

where $i = \sqrt{-1}$, $S(\boldsymbol{r})$ is the source distribution (normally called the initial pressure distribution) which is contained within a circular ball $B^2_{r_0}$ with bounding radius of r_0, $\boldsymbol{r} \triangleq (r, \phi)$ is the position vector of the source with r the radial and ϕ the angular coordinate, $k = 2\pi f/c$ is the wavenumber with f the frequency and c the speed of sound waves, and the 2D Green's function $G(k; (r_s, \phi_s), \boldsymbol{r}) \triangleq i/4H_0^{(1)}(k\|(r_s, \phi_s) - \boldsymbol{r}\|)$ with $H_0^{(1)}(\cdot)$ is the zeroth order Hankel function of the first kind and $\|\cdot\|$ is the l_2 norm.

Photoacoustic inversion requires finding the source distribution $S(\boldsymbol{r})$ from the measured pressure. Writing (1) with operator notation $p(\phi_s, k) = (\mathcal{M}S)(\phi_s, k) + n(\phi_s, k)$ where the operator $\mathcal{M}$ links the source distribution to the measured pressure according to (1) and $n(\phi_s, k)$ is additive, zero mean, white Gaussian noise with variance of σ_n^2. Let the vector $\boldsymbol{p} \in \mathbb{R}^U$ contain all the measured pressure at all angles and frequency, $\boldsymbol{S} \in \mathbb{R}^{P\times Q}$ be the discrete version of $S(\boldsymbol{r})$ and $\boldsymbol{x} = \mathrm{vec}(\boldsymbol{S})$ with $\mathrm{vec}(\cdot)$ the column stacking operator. The photoacoustic inversion problem in matrix notation is $\boldsymbol{p} = \boldsymbol{M}\boldsymbol{x} + \boldsymbol{n}$ where $\boldsymbol{n}$ is the noise vector and $\boldsymbol{M}$ is the sensitivity matrix mapping $\boldsymbol{x}$ to $\boldsymbol{p}$.

The constrained TV formulation minimizes $\mathrm{TV}(\boldsymbol{S})$ subject to the fidelity constraint (A): $\|\boldsymbol{p} - \boldsymbol{M}\boldsymbol{x}\|^2 \leq U\sigma_n^2$ and the non negativity constraint (B): $\boldsymbol{S} \geq 0$, where $\mathrm{TV}(\boldsymbol{S}) = \sum_{p=1}^{P-1}\sum_{q=1}^{Q-1}\{|\boldsymbol{S}_{p,q} - \boldsymbol{S}_{p+1,q}| + |\boldsymbol{S}_{p,q} - \boldsymbol{S}_{p,q+1}|\} = \|\boldsymbol{D}\boldsymbol{x}\|_1$. This is known as the l_1 based anisotropic TV where $\|\cdot\|_1$ is the l_1 norm and $\boldsymbol{D}$ is a suitable difference matrix. In this form, the TV minimization method works with a large amount of data. Projection onto the ellipsoidal, fidelity constraint requires solving an SOCP. Moreover, reconstruction methods such as [4, 5] cannot be adapted for TV minimization. This paper uses a Frequency-Radial duality (F-R) based ideas described in [2, 3] for TV minimization.

3. F-R BASED RECONSTRUCTION

The normalized Fourier Bessel series

$$\Psi_{m\ell} \triangleq \frac{1}{\sqrt{\pi}} \frac{1}{r_0 J_{m+1}(z_{m\ell})} J_m(r\, z_{m\ell}/r_0) e^{im\phi} \qquad (2)$$

where m denotes the mode, ℓ the zero index, $J_m(\cdot)$ is the m^{th} order Bessel function and $z_{m\ell}$ is the ℓ^{th} root of $J_m(\cdot)$, is a complete orthonormal basis for $L^2(B_{r_0}^2)$ with inner product $\langle S(\boldsymbol{r}), f(\boldsymbol{r})\rangle = \int_0^{2\pi}\int_0^{r_0} S(\boldsymbol{r}) f(\boldsymbol{r})^* r\, \mathrm{d}r\, \mathrm{d}\phi$, $(\cdot)^*$ is the complex conjugate operator (discrete version of this inner product can be done using numerical integration methods such as the trapezoidal method thus replacing integrals with sums). The source distribution $S(\boldsymbol{r}) \in L^2(B_{r_0}^2)$ can be expanded with these basis functions (synthesis equation) as $S(\boldsymbol{r}) = \sum_{m=-\infty}^{\infty}\sum_{\ell=1}^{\infty} \beta_{m\ell}\Psi_{m\ell}$ where $\beta_{m\ell}$ is a complex, Fourier Bessel coefficient. The F-R based method calculates $\beta_{m\ell}$ from the modal expansion of the aperture function defined as

$$a_m(k) = (\mathcal{A}_m p)(k) = \frac{1}{\sqrt{2\pi}} \int_0^{2\pi} p(\phi_s, k) e^{-im\phi_s}\, \mathrm{d}\phi_s \quad (3)$$

where $a_m(k)$ is called the modal coefficient and $\mathcal{A}$ is an operator defined in (3). We note that the functions $\{1/\sqrt{2\pi}e^{im\phi_s}\}$ forms a complete, orthonormal basis for integrable functions on the unit circle $\mathbb{S}$ i.e. $L^2(\mathbb{S})$. The Fourier Bessel coefficients are estimated by $\beta_{m\ell} = h_{m\ell} a_{m\ell}$ where $a_{m\ell} = a_m(k)|_{k=z_{m\ell/r_0}}$ and the weighting factor

$$h_{m\ell} = \frac{2\sqrt{2}}{\pi c\, z_{m\ell} J_{m+1}(z_{m\ell})\, H_m^{(1)}(r_s z_{m\ell}/r_0)}. \qquad (4)$$

From $\beta_{m\ell}$, the source distribution $S(\boldsymbol{r})$ can be reconstructed by the synthesis equation.

In practice, the measurement bandwidth is finite with a lower frequency limit of k_l and an upper frequency limit of k_u, then the set of the coefficients which can be recovered are $\Lambda = \{m, \ell | k_l \leq z_{m\ell/r_0} \leq k_u, l \geq 1, m \in \mathbb{Z}, l \in \mathbb{Z}\}$. Therefore, an index limited source distribution is recovered,$(\mathcal{B}_\Lambda S)(\boldsymbol{r}) = \sum_{\{m,\ell\}\in\Lambda}\langle S(\boldsymbol{r}), \Psi_{m\ell}\rangle \Psi_{m\ell}$. The complement of this index limiting operator is $(\mathcal{B}_{\Lambda^C} S)(\boldsymbol{r}) = S(\boldsymbol{r}) - (\mathcal{B}_\Lambda S)(\boldsymbol{r})$ where Λ^C is the complement of set Λ.

4. TV FORMULATION IN THE FOURIER BESSEL DOMAIN

The following theorem proves the noise power remains unchanged in the modal domain.

Theorem 1 *[White Gaussian Noise in L^2] Given a zero, mean white Gaussian noise with variance σ_n^2 in $L^2(\breve{\Omega})$ represented by a random variable $n(\boldsymbol{r})$ where $\boldsymbol{r} \in \breve{\Omega} \subseteq \mathbb{R}^U$, such that for any function $\Psi_i(\boldsymbol{r}) \in L^2(\breve{\Omega})$ the complex scalar n_i*

$$n_i \triangleq \int_{\breve{\Omega}} n(\boldsymbol{r})\Psi_i(\boldsymbol{r})^*\, \mathrm{d}\boldsymbol{r} = \langle n(\boldsymbol{r}), \Psi_i(\boldsymbol{r})\rangle$$

is also a zero mean, Gaussian random variable with variance $E(|n_i|^2) = \sigma_n^2 \int_{\breve{\Omega}} |\Psi_i(\boldsymbol{r})|^2\, \mathrm{d}\boldsymbol{r} = \sigma_n^2(\|\Psi_i(\boldsymbol{r})\|_{L^2})^2$. [6, eqn 8.1.35].

When the function $\Psi_i(\boldsymbol{r})$ are orthonormal, $\boldsymbol{n} = \{n_i\}_{i=-\infty}^{\infty}$ are a vector of *i.i.d.*, zero mean, Gaussian random variable with variance σ_n^2. From Theorem 1, the orthonormal, modal expansion of the noise at mode m, $(\mathcal{A}_m\, n)(z_{m\ell}/r_0)$ remains a zero mean Gaussian random variable with variance σ_n^2.

4.1. Reduced Dimension Fidelity Constraint

Let the actual Fourier Bessel coefficients be denoted by $\beta_{m\ell}$ and those estimated using the measured pressure be $\widetilde{\beta}_{m\ell}$. Then the calculated modal coefficients are $\widetilde{a}_{m\ell} = \widetilde{\beta}_{m\ell}/h_{m\ell}$ and the actual modal coefficients are $a_{m\ell} = \beta_{m\ell}/h_{m\ell}$. Since all the information of the source distribution can be obtained from modal coefficients at the frequencies corresponding to the roots of Bessel functions, the fidelity constraint can now be written in the modal domain as: $\sum_{\{m,\ell\}\in\Lambda}|a_{m\ell} - \widetilde{a}_{m\ell}|^2 \leq \mathrm{card}(\Lambda)\sigma_n^2$. This results in a large reduction of dimension for the fidelity constraint. where $\mathrm{card}(\Lambda)$ is the cardinality operator returning the number of elements in set Λ.

Since $S(\boldsymbol{r})$ is a real function then $\beta_{(-m)\ell} = \beta_{m\ell}^*$ [3]. Further, $h_{(-m)\ell} = h_{m\ell}$ if we use the following identities

$H_{-m}(\cdot) = (-1)^m H_m(\cdot)$ and
$J_{-m+1}(z_{m\ell}) = (-1)^m J_{m+1}(z_{m\ell})$ in (4). Subsequently,

$$|a_{(-m\ell)} - \widetilde{a}_{(-m\ell)}| = \left| \frac{h^*_{m\ell}}{h_{m\ell}}\, a^*_{m\ell} - \frac{h^*_{m\ell}}{h_{m\ell}}\, \widetilde{a}^*_{m\ell} \right| = |a_{(m\ell)} - \widetilde{a}_{(m\ell)}| \tag{5}$$

since $|h^*_{m\ell}/h_{m\ell}| = 1$. Therefore, the fidelity constraint (A), becomes:

$$\|\boldsymbol{a} - \widetilde{\boldsymbol{a}}\|^2 \leq \mathrm{card}(\tilde{\Lambda})\sigma_n^2 \tag{6}$$

where the set $\tilde{\Lambda} = \{m, \ell | \{m, \ell\} \in \Lambda, m \geq 0\}$ and contains only the zeroth and positive modes, $\widetilde{\boldsymbol{a}}$ is a vector of calculated modal coefficients $\widetilde{a}_{m\ell}$ and $\boldsymbol{a}$ is a vector of the actual modal coefficients $a_{m\ell}$ for $\{m, \ell\} \in \tilde{\Lambda}$. The cardinality of the new set $\tilde{\Lambda}$ is half the previous set Λ. Therefore, working in the modal domain reduces the dimension of the fidelity from the first TV formulation.

5. SUBGRADIENT BASED ALGORITHM

The TV minimization problem can set as: minimize $\mathrm{TV}(\boldsymbol{S})$ subject to $\boldsymbol{S} \in \mathcal{C}$ where $\mathcal{C}$ is a convex set. We choose to apply subgradient based method since this method is scalable to large data sets. This minimization is achieved by the projected subgradient method, with the iteration

$$\boldsymbol{S}^{(\kappa+1)} = \mathscr{P}_{\mathcal{C}}(\boldsymbol{S}^{(\kappa)} - \gamma_\kappa \boldsymbol{g}^{(\kappa)}_{\mathrm{TV}}) \tag{7}$$

where $\boldsymbol{S}^{(\kappa)}$ solution at the κ^{th} iterate, γ_κ is the κ^{th} step size, $\boldsymbol{g}^{(\kappa)}_{\mathrm{TV}}$ is any subgradient of $\mathrm{TV}(\cdot)$ at $\boldsymbol{S}^{(\kappa)}$ and $\mathscr{P}_{\mathcal{C}}$ is the projection onto $\mathcal{C}$. The starting value $\boldsymbol{S}^{(0)}$ is the reconstructed image from the F-R based method with a projection onto the non negativity constraint. The subgradient is taken as $\boldsymbol{g}^{(\kappa)}_{\mathrm{TV}} = \boldsymbol{D}^T \mathrm{sgn}(\boldsymbol{D}\boldsymbol{x}^{(\kappa)})$ and $\mathrm{sgn}(\boldsymbol{x})$ for a vector $\boldsymbol{x}$ is a vector of equal dimensions whose co-ordinates are the signs of the corresponding co-ordinates in $\boldsymbol{x}$. The step sizes are chosen as $\gamma_\kappa = D/(\kappa + 1)$ where D is a constant set a priori by the user. These step sizes are a class of step sizes that are square summable but not summable. The convergence proof for these types of step sizes is shown in [7]. Moreover, the number of iterations to be performed is set a priori by the user.

The operator $\mathscr{P}_B$ for projection onto the non negativity constraint simply sets all negative values to zero in the source distribution. Transforming into the Fourier Bessel domain makes the fidelity constraint (A) into a spheroidal constraint. The projection onto this constraint (projection onto an l^2 ball) can be done by the following projection operator

$$(\tilde{\mathscr{P}}_A\, \boldsymbol{a}) = \begin{cases} \boldsymbol{a} & \text{if } \|\boldsymbol{a} - \widetilde{\boldsymbol{a}}\|^2 \leq \mathrm{card}(\tilde{\Lambda})\sigma_n^2 \\ \widetilde{\boldsymbol{a}} + \boldsymbol{\upsilon} & \text{otherwise} \end{cases} \tag{8}$$

where the vector $\boldsymbol{\upsilon} = \frac{\boldsymbol{a} - \widetilde{\boldsymbol{a}}}{\|\boldsymbol{a} - \widetilde{\boldsymbol{a}}\|} \sqrt{\mathrm{card}(\tilde{\Lambda})}\, \sigma_n$. The projection operator $\boldsymbol{a}' = (\tilde{\mathscr{P}}_A\, \boldsymbol{a})$ results in a new set of modal coefficients $\boldsymbol{a}'$ from which a new set of Fourier Bessel coefficients $\beta'_{m\ell}$ can be obtained. Therefore, this projection changes the source distribution according to $(\mathscr{P}_A\, \boldsymbol{S}) = (\mathscr{B}_{\Lambda^C}\, \boldsymbol{S}) + \sum_{\{m,\ell\} \in \Lambda} \beta'_{m\ell} \Psi_{m\ell}$. Note that $\boldsymbol{a}$ changes with each iteration as the source distribution changes. However, $\widetilde{\boldsymbol{a}}$ remains constant.

5.1. Dealing with Multiple Convex Constraints

We define a mapping or operator $\mathscr{T} : \mathcal{H} \to \mathcal{H}$ on an Hilbert space $\mathcal{H}$ as non-expansive if it satisfies the following property $|\mathscr{T}(\boldsymbol{x}) - \mathscr{T}(\boldsymbol{y})\| \leq \|\boldsymbol{x} - \boldsymbol{y}\|$ for $\forall\, \boldsymbol{x}, \boldsymbol{y} \in \mathcal{H}$. The projection operators $\mathscr{P}_A$ and $\mathscr{P}_B$ are non-expansive mappings. Now to project onto the intersection of both these convex sets $\mathcal{C} = A \cap B$ requires several alternative projections where the computational complexity of projection operator $\mathscr{P}_A$ is equal to computational complexity of Fourier Bessel transform, i.e., $\mathcal{O}(Q^2 \log Q)$ for $\boldsymbol{S} \in \mathbb{R}^{Q \times Q}$. Therefore, several projections for one iteration is computationally expensive.

Lets define the operator $(\mathscr{P}_{\mathcal{C}}) \triangleq (\mathscr{P}_B \circ \mathscr{P}_A \boldsymbol{S})$. Given $\boldsymbol{T} \in \mathcal{C}$, then since $\boldsymbol{T} \in A$, we have $\|(\mathscr{P}_A \boldsymbol{S}) - \boldsymbol{T}\| \leq \|\boldsymbol{S} - \boldsymbol{T}\|$ and since $\boldsymbol{T} \in B$ also, we have $\|(\mathscr{P}_B \circ \mathscr{P}_A \boldsymbol{S}) - \boldsymbol{T}\| \leq \|(\mathscr{P}_A \boldsymbol{S}) - \boldsymbol{T}\|$. Combining both these inequalities, the new operator has the following property $\|(\mathscr{P}_{\mathcal{C}} \boldsymbol{S}) - \boldsymbol{T}\| \leq \|\boldsymbol{S} - \boldsymbol{T}\|$ and only requires one projection for each set. The operator $\mathscr{P}_{\mathcal{C}}$ is a non-expansive mapping. The proof of convergence using this method proceeds in the same way as the convergence proof for the projected, subgradient method shown in [7].

The F-R based reconstruction for the circular geometry have a computational order of $\mathcal{O}(Q^2 \log Q)$. The use of the TV minimization methods proposed in this paper will not change the computational complexity of the F-R based method provided the number of iterations chosen $\mathcal{K}$ is small, i.e., $\mathcal{K} \ll Q$. However, compared to the standard F-R based method, the amount of computations increases with the number of iterations $\mathcal{K}$.

6. SIMULATIONS

Numerical experiments were performed to investigate the improvements in the image quality after applying the proposed TV minimization method to the reconstructed images from an F-R based reconstruction method. The numerical phantom used in the simulations is shown in Fig. 1a. The signals generated by the circular discs were produced according to the formula described in [8]. The speed of sound c was set at 1500 m/s which is the speed of sound in biological tissue. Both the bounding radius r_0 and the sensor radius r_s was set to 10 mm. Noise was added to the generated pressure signals according to SNR $= 10 \log_{10}(\int_0^{T_s} |p(\boldsymbol{r}_{ref}, t)|^2\, \mathrm{d}t/(T_s \sigma_n^2))$ where the reference sensor is the sensor placed at a angular position $\phi = 0$ and T_s is total amount of time for which the

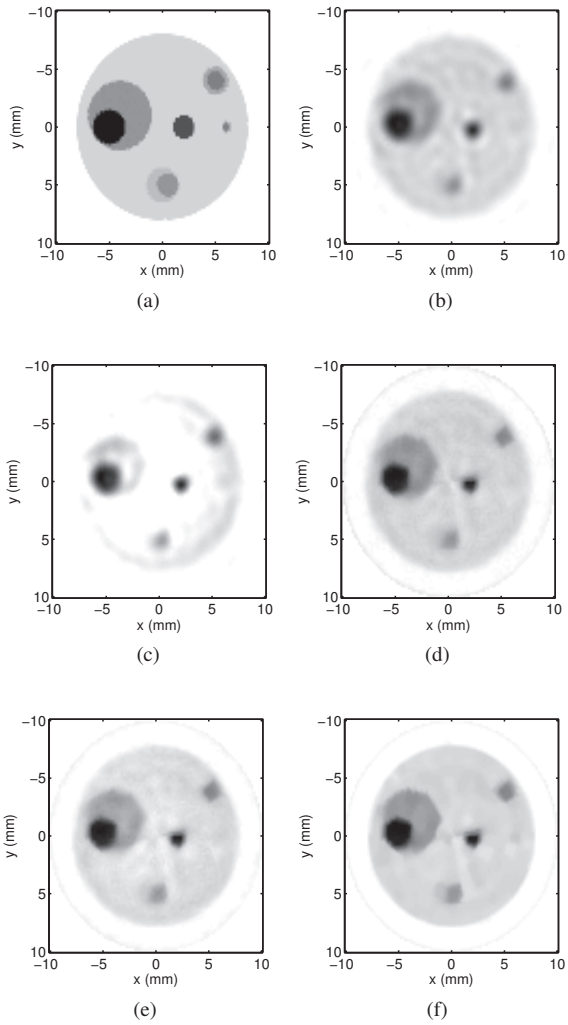

Fig. 1. (a) The numerical phantom. F-R based reconstructions (b) bandwidth from 0 to 1 MHz and (c) bandwidth from 100 KHz to 1 MHz. Resulting image after TV minimization method (d) after 10 iterations for measurement bandwidth from 0 to 1 MHz and for measurement bandwidth from 100 KHz to 1 MHz (e) after 10 iterations and (f) after 50 iterations.

signals are recorded. In the numerical experiments, 20 dB of noise was added to the generated signals.

The reconstructed images from applying the F-R based reconstruction method to the generated data for different measurement bandwidths are shown in Fig. 1b and Fig. 1c. We observe that large structures are not fully reconstructed when the lower frequency limit is larger than zero. The step size constant D was chosen to be 0.1 in the numerical experiments. The resulting images after TV minimization are shown in Fig. 1e, Fig. 1f and Fig. 1d. Most of the improvements occurred in the first few iterations. The TV minimization method is capable of recovering the lost, low frequency information and removes ripply artifacts. Furthermore, the TV minimization method provides more improvement when the lower frequency limit of measurement is higher than zero and allows better identification of the different discs in the numerical phantom.

7. CONCLUSION

We have proposed a subgradient based TV minimization for photoacoustic tomography capable of dealing with large data sets. Further, by working in the Fourier Bessel domain a constrained TV formulation is possible since the projection onto the fidelity constraint can be performed by a simple projection onto the l_2 ball. The TV minimization postprocessing produces better quality reconstruction with a few number of iterations than only using the F-R based reconstruction. Possible applications include cancer detection, imaging blood vessels and photoacoustic microscopy.

8. REFERENCES

[1] A.H. Delaney and Y. Bresler, "Globally convergent edge-preserving regularized reconstruction: an application to limited-angle tomography," *Image Processing, IEEE Transactions on*, vol. 7, no. 2, pp. 204–221, 1998.

[2] S. M. A. Salehin and T. D. Abhayapala, "Photoacoustic image reconstruction from a frequency-invariant source localization perspective," in *European Signal Processing Conference (EUSIPCO)*, 2010.

[3] S. M. A. Salehin and T. D. Abhayapala, "Frequency domain, photoacoustic tomography with sparse frequency samples," in *Signal Processing Systems (SIPS), 2010 IEEE Workshop on*. IEEE, 2010, pp. 260–265.

[4] S.J. Norton and M. Linzer, "Ultrasonic reflectivity imaging in three dimensions: exact inverse scattering solutions for plane, cylindrical, and spherical apertures," *Biomedical Engineering, IEEE Transactions on*, , no. 2, pp. 202–220, 1981.

[5] M. Xu and L. V. Wang, "Time-domain reconstruction for thermoacoustic tomography in a spherical geometry," *Medical Imaging, IEEE Transactions on*, vol. 21, no. 7, pp. 814–822, 2002.

[6] R. Gallager, *Information Theory and Relaible Communication*, New York, USA: John Wiley & Sons, 1968.

[7] N. Z. Shor, *Minimization methods for non-differentiable functions*, Springer-Verlag, Berlin, 1985.

[8] G. J. Diebold, T. Sun, and M. I. Khan, "Photoacoustic monopole radiation in one, two, and three dimensions," *Phys. Rev. Lett.*, vol. 67, no. 24, pp. 3384–3387, Dec 1991.